Misoprostol Attenuates Cardiomyocyte Proliferation in the Neonatal Heart through Bnip3 and Perinuclear Calcium Signaling

Matthew D. Martens[1,5], Jared T. Field[1,5], Donald Chapman[5], Adrian R. West[2,6], Tammy L. Ivanco[4], and Joseph W. Gordon[1,3,5,6,*]

Departments of Human Anatomy and Cell Science[1], Physiology[2], and the College Nursing[3] in the Rady Faculty of Health Science, The Department of Psychology[4] in the Faculty of Arts, The Diabetes Research Envisioned and Accomplished in Manitoba (DREAM) Theme[5] and the Biology of Breathing (BoB) Theme[6] of the Children's Hospital Research Institute of Manitoba, University of Manitoba, Winnipeg, Canada.

Running title: Misoprostol opposes hypoxia-induced cardiomyocyte proliferation

*Corresponding Author:

Children's Hospital Research Institute of Manitoba, Diabetes Research Envisioned and Accomplished in Manitoba (DREAM) research group

Department of Human Anatomy and Cell Science

College of Nursing, Rady Faculty of Health Sciences,

University of Manitoba.

715 McDermot Avenue, Winnipeg

Phone: 204-474-1325

Fax: 204-474-7682

joseph.gordon@umanitoba.ca

Misoprostol opposes hypoxia-induced cardiomyocyte proliferation

Abstract:

Systemic hypoxia resulting from preterm birth, altered lung development, placental abnormalities, and cyanotic congenital heart disease is known to impede the regulatory and developmental pathways in the neonatal heart. While the molecular mechanisms are still unknown, stressors that result from systemic hypoxia drive aberrant cardiomyocyte proliferation, which may be initially adaptive, but ultimately can program the heart to fail in early life. Recent evidence suggests that the prostaglandin E1 analogue, misoprostol, is cytoprotective in the hypoxia-exposed neonatal heart by impacting alternative splicing of the BCL-2/adenovirus E1B 19 kd-interacting protein 3 (Bnip3) resulting in the generation of an isoform lacking the third exon (Bnip3ΔExon3) or small Nip (sNip). Using a rodent model of neonatal hypoxia, in combination with rat primary ventricular neonatal cardiomyocytes (PVNC's) and H9c2 cells, we sought to determine if misoprostol can prevent cardiomyocyte proliferation and what the key molecular mechanisms might be in this pathway. At postnatal day (PND) 10, hypoxia-exposed rat pups demonstrated elevated heart weights, while histological analysis confirmed increased nuclei number and the absence of fibrosis ($P<0.05$), which was completely attenuated with the addition of 10 μg/kg/day misoprostol. Concurrently, molecular markers of proliferation, including Cyclin-D1 were significantly elevated in hypoxia-exposed myocytes, which was also prevented in the presence of misoprostol ($P<0.05$). We further describe a critical role for sNip in the regulation of cardiomyocyte proliferation at the transcriptional level, where this isoform reduced the expression of a proliferative MEF2C-myocardin-BMP10 pathway, while favoring expression of the cardiac maturation factors, such as BMP2 and MEF2A. These observations were further supported with knockdown studies in H9c2 cells, where we are able to restore hypoxia-induced cardiomyocyte proliferation in misoprostol-treated cells with the addition of an siRNA targeting sNip. Taken together this data demonstrates a mechanism for hypoxia-induced neonatal cardiomyocyte proliferation which can pharmacologically mitigated by misoprostol treatment.

Introduction:

Neonatal systemic hypoxia resulting from early-life cyanotic events including preterm birth, placental abnormalities, abnormal/impaired lung development, and certain forms of congenital heart disease, are known drivers of both structural and functional changes in the developing heart (3, 5). Specifically, these infants demonstrate dramatic reductions in systolic and diastolic function, concurrent with extensive increases in left-ventricular mass (25). While such changes are thought to be initially protective to preserve cardiac output in the neonatal stage, they also significantly increase the risk for pediatric heart failure, and lifelong cardiovascular abnormalities (3, 25, 36).

Although traditional literature suggests that cardiomyocytes proliferate early in gestation, and that postnatal cardiac growth is achieved exclusively through hypertrophy, recent evidence in humans demonstrates that cardiomyocytes continue to proliferate in the first year of life, and a small number remain proliferative for as long as 20 years (40). Moreover in rodents, the cardiomyocyte is able to retain its ability to proliferate until the point of binucleation, which occurs on or before postnatal day 7 (35). Work focused specifically on this developmental window of proliferation has further revealed that cardiomyocytes continue to undergo mitosis longer in an environment where the oxygen tension is low, even extending into adulthood, where whole animal hypoxia-exposure following myocardial infarction, reduces cardiac damage and fibrosis, by enhancing cardiomyocyte proliferation (20, 33, 40).

The developmental switch from proliferation to hypertrophy is the result of large-scale shifts in gene expression; however, changes in the expression pattern of the myocyte enhancer factor-2 (MEF2) family appears to be a key event (9, 10, 26, 32). Genetic studies have shown that three MEF2 genes have non-redundant and potentially antagonistic roles in proliferation (MEF2C), differentiation (MEF2A), and maturation (MEF2D) (10, 19, 26, 32, 34). These developmentally programmed roles of the MEF2 family converge on Notch signaling, to drive the expansion of cardiomyocytes and simultaneously promote maturation (8, 10). Furthermore, MEF2C expression is governed by hypoxia signalling, where loss of the hypoxia-inducible factor-1α (HIF1α) prevents MEF2C expression, cardiac looping and embryo viability (2, 23).

Myocardin, a transcriptional co-activator involved in the determination, differentiation and maturation of cardiomyocytes, is a direct transcriptional target of MEF2C, while simultaneously being a positive co-activator of MEF2C-dependent gene expression in the heart (10, 19, 23, 34). This regulatory cycle is further complicated by bone morphogenetic protein (BMP) 10, a growth factor associated with embryonic cardiomyocyte proliferation, which is positively regulated by a myocardin-serum response factor (SRF) complex, but is itself a driver of MEF2C expression (5, 13, 18, 31).

In contrast to proliferation, cardiomyocyte hypertrophy signaling is largely dominated by the calcium-calmodulin-dependent phosphatase, calcineurin (PP2B) (29, 30, 42, 48). Classically, calcineurin is activated by low amplitude nuclear calcium transients, resulting in nuclear accumulation of nuclear factor of activated T-Cells (NFAT) (6, 29). In the nucleus, NFATs complex with GATA4 to drive the expression of many hypertrophy genes including beta-myosin heavy chain (β-MHC), brain natriuretic peptide (BNP), myocyte-enriched calcineurin-interacting protein 1 (MCIP1), and endothelin 1 (ET-1) [Reviewed by Wilkins and Molkentin, 2002 (42)]. In addition to its interactions with GATA4, NFAT also physically interacts with the p65 subunit of nuclear factor kappa B (NF-κB) and is able to drive differentiation, hypertrophy and eventually pathological remodeling of the ventricle (12). Additionally, calcineurin has been shown to enhance MEF2A activity (43, 44).

Independent from the hypoxia-inducibility of MEF2C, HIF1α also drives the expression of BCL2/Adenovirus E1B 19 KDa Protein-Interacting Protein 3 (Bnip3), whose protein products play a pivotal role in hypoxia-induced cardiomyocyte apoptosis, necrosis and autophagy (1, 16, 17, 22, 24, 38, 39). Alternative splicing of Bnip3 produces a truncated form of the protein (ie. short/small Nip or sNip) lacking the second exon in humans, or the third exon in rodents, that acts as an endogenous inhibitor of the full-length protein (13, 14). Recently, we have shown that these spliced variants also drive the accumulation of calcium in the nucleus triggering hypertrophic growth of cardiomyocytes. Interestingly, we also demonstrated that the prostaglandin analogue, misoprostol can modulate the expression of sNip in multiple cell and tissue types (11, 13).

Building on this previous work, in this report we provide evidence that hypoxia drives proliferation in the neonatal heart, primary ventricular neonatal cardiomyocytes and cultured cell lines in a MEF2C/BMP10-dependent manner**.** We further show that hypoxia in combination with misoprostol treatment, enhances sNip expression and nuclear calcium retention, opposing hypoxia-induced proliferation, while promoting maturation and hypertrophy.

Materials and Methods:

In vivo neonatal hypoxia model:

All procedures in this study were approved by the Animal Care Committee of the University of Manitoba, which adheres to the principles for biomedical research involving animals developed by the Canadian Council on Animal Care. Litters of Long-Evans rat pups and their dams were placed in a hypoxia chamber with 10% O_2 (±1%) from postnatal day (PND) 5-10. Additionally, hypoxic animals were exposed to 100% N_2 for 90 seconds, daily from PND 5-7 (inclusive). Control litters (N=3), were left in normoxic conditions at 21% O_2. Animals received 10 µg/kg misoprostol or saline control, administered orally in rat milk substitute daily from PND5-10. At PND10 animals were euthanized and perfused with saline for tissue collection.

Histology:

Male PND10 hearts were fixed in 10% buffered formalin for 24 hours at time of sacrifice and stored in phosphate buffered saline (PBS; Hyclone). Fixed hearts were cut longitudinally (to expose the four chambers of the heart), processed and embedded in paraffin blocks. Hearts were sectioned at 5µm thicknesses, mounted on APTES coated slides, and stained with Hematoxylin and Eosin or Masson's Trichome by the University of Manitoba Histology Core. Hearts were imaged on a on a Zeiss Axio Lab.A1 bright-field microscope fitted with an Axiocam 105 color camera (Zeiss). Imaging was done using Zen 2.3 Pro imaging software and quantification, scale bars, and processing was done on Fiji (ImageJ) software.

Plasmids and virus production:

The endoplasmic reticulum (CMV-ER-LAR-GECO1), and nuclear (CMV-NLS-R-GECO) targeted calcium biosensors were gifts from Robert Campbell (Addgene #61244, and 32462) (45, 46).

CMV-dsRed was a gift from John C. McDermott and myc-NFATc3 was a gift from Tetsuaki Miyake. The mouse HA-Bnip3ΔExon3 (sNip) (Accession #MF156210) were described previously (Addgene #100793) (11). Generation of the pLenti-Bnip3ΔExon3 (sNip) virus using a pLenti-puro back bone, which was described previously (13).

Cell culture, transduction and transfections:

Rat primary ventricular neonatal cardiomyocytes (PVNC) were isolated from 1-2-day old pups using the Pierce Primary Cardiomyocyte Isolation Kit (#88281). H9c2 cells were maintained in Dulbecco's modified Eagle's medium (DMEM; Hyclone), containing penicillin, streptomycin, and 10% fetal bovine serum (Hyclone), at 37 °C and 5% CO2. All cells were transfected using JetPrime Polyplus reagent, as per the manufacturer's protocol. Lentiviral expression of sNip and RNAi targeting of sNip were described previously (13). For misoprostol treatments, 10 mM misoprostol (Sigma) in phosphate buffered saline (PBS; Hyclone) was diluted to 10 μM directly in media and applied to cells for 48 hours. For hypoxia treatments, cells were held in a Biospherix incubator sub-chamber with 10% O_2 (±1%), 5% CO_2, balanced with pure N_2 (regulated by a Biospherix ProOx C21 sub-chamber controller) at 37 °C for 48 hours.

Fluorescent staining, live cell imaging and immunofluorescence:

Hoechst 3334 and Calcein-AM were all purchased from Biotium and applied using manufacturer's protocol. Tag-it Violet Proliferation and Cell Tracking Dye was purchased from BioLegend and applied using the manufacturer's protocol. Immunofluorescence with Anti-NF-kB (CST #8242) and Myc-Tag (CST # 2272) were used with fluorescent secondary antibody conjugated to Alexa Fluor 466 (Jackson #711-545-152) in fixed and permeabilized PVNC's and H9c2's. All imaging experiments were done on a Zeiss Axiovert 200 inverted microscope fitted with a Calibri 7 LED Light Source (Zeiss) and Axiocam 702 mono camera (Zeiss). Imaging was done using Zen 2.3 Pro imaging software and quantification, scale bars, and processing including background subtraction, was done on Fiji (ImageJ) software.

Measurement of Proliferation by Flow Cytometry:

Cell cycle was assessed by flow cytometry using the Nicoletti method and FxCycle™PI/RNase Staining Solution purchased from Invitrogen (product # F10797) (41). Red fluorescence was analyzed for

20,000 cells/treatment using a Thermo Scientific Attune NxT flow cytometer equipped with a 488 nm laser, as per the manufacturer's protocol. Gating and DNA histogram analysis was described previously (28).

Immunoblotting:

Protein isolation and quantification was performed as described previously (3). Extracts were resolved via SDS-PAGE and later transferred to a PVDF membrane using an overnight transfer system. Immunoblotting was carried out using primary antibodies in 5% powdered milk or BSA (as per manufacturer's instructions) dissolved in TBST. Horseradish peroxidase-conjugated secondary antibodies (Jackson ImmunoResearch Laboratories; 1:5000) were used in combination with enhanced chemiluminescence (ECL) to visualize bands. The following antibodies were used: Myocardin (sc-33766), Cyclin-D1 (sc-450), p57(KP39) (sc-56341), MEF2C (CST #5030), MEF2A (CST #9736), Myc-Tag (CST # 2272), NFATc3 (F-1) (sc-8405), p-NFATc3 (Ser 169) (sc-68701), Histone-H3 (CST #4499), MEK1/2 (CST #8727), Actin (sc-1616), and Tubulin (CST #86298). For detection of the Bnip3 splice variant, Bnip3ΔExon3 (sNip), we used a custom rabbit polyclonal antibody that was previously described and validated (3).

Real-Time PCR:

Total RNA was extracted from cells and pulverized tissues by the TRIzol extraction method and genomic DNA was removed via the RNeasy Mini Kit (Qiagen), including an On-Colum DNase Digestion (Qiagen). For qRT-PCR, mRNA was extracted from cells using Trizol then reverse transcribed into cDNA. Following DNase treatment, cDNA was combined with SYBR Green Supermix (Thermo) and mRNA was amplified using the ABI 7500 Real-Time PCR system (Applied Biosystems). Primers were: MEF2C Mus Fwd: GATGCAGACGATTCAGTAGGTC, MEF2C Mus Rev: GGATGGTAACTGGCATCTCAA, MEF2A Rat FWD: GGAACCGACAGGTGACTTTTA, MEF2A Rat REV: AGAGCTGTTGAAGATGATGAGTG, BMP10 Rat Fwd: TGCCATCTGCTAACATCATCC, BMP10 Rat Rev: CAAACGATCTCTCTGCACCA, BMP2 Rat FWD: GCTCAGCTTCCATCACGAA, BMP2 Rat REV: GAAGAAGCGTCGGGAAGTT, MYOCD Rat Fwd: GTGTGGAGTCCTCAGGTCAAAC,

MYOCD Rat Rev: TGATGTGTTGCGGGCTCTT, L13 Rat Fwd: AGGAGGCGAAACAAATCCAC, L13 Rat Rev: TATGAGCTTGGAGCGGTACTC.

Statistics:

Data are presented as mean ± standard error (S.E.M.). Differences between groups in imaging experiments with only 2 conditions were analyzed using an unpaired t-test, where (*) indicates $P<0.05$ compared with control. Experiments with 4 or more conditions were analyzed using a 1-way ANOVA, with Newman-Keuls test for multiple comparisons, where (*) indicates $P<0.05$ compared with control, and (**) indicates $P<0.05$ compared with treatment. All statistical analysis was done using GraphPad Prism 6 software.

Results:

Misoprostol opposes hypoxia-induced neonatal cardiomyocyte proliferation

Hypoxia exposure in the developing, and not yet terminally differentiated cardiomyocyte, has been previously linked with the initiation of the cell cycle and proliferation (35). In addition, we have previously observed that PGE1 signalling, activated by misoprostol, is cardioprotective through a mechanism contingent on the expression of a small alternative spliced Bnip3 isoform, called sNip (13). Therefore, we tested the hypothesis that misoprostol could be further cardioprotective in the neonatal heart, by attenuating cardiomyocyte proliferation through a sNip-dependent mechanism.

To test this we used a rodent model of neonatal hypoxia, and observed that hypoxic animals demonstrated significantly elevated heart weights compared to control, an increase that was absent in hypoxia and misoprostol treated animals (Fig. 1, A). Histological examination of the neonatal left ventricle confirmed this hypoxia-induced increase in heart weight was not due to fibrosis, but rather an increase in the number of nuclei present, by an average of 9.5 nuclei per field. Importantly, in hypoxia and misoprostol treated animals, the average number of nuclei was not elevated beyond control (Fig. 1, B & C). Biochemically, we also assessed cyclin-D1 expression, a protein rapidly accumulates in the G_1 phase of the cell cycle and is further required for the transition from the G_1 to S phase. Interestingly, we observed no significant hypoxia-induced change from control, but the combination of hypoxia and misoprostol, reduced

cyclin-D1 expression by more than 65%, the first indicator that the combination of hypoxia and misoprostol may actually be suppressing the cell cycle (Fig. 1, D).

In order to explore this mechanism further, we employed cultured primary ventricular neonatal cardiomyocytes (PVNC's), isolated from PND 1-2 rats pups, closely mirroring our animal model. Here, we show that 48-hours at 10% O_2 is sufficient to drive cyclin-D1 expression well over that of normoxic control cells, which was completely absent with the addition of misoprostol (Fig. 1, E). Using live cell imaging we observed that hypoxia significantly elevates the number of proliferative PVNC's compared to control, which is partially rescued with the addition of misoprostol (Fig. 1, F & G). To confirm that this hypoxia-induced proliferation was also happening at the cell population level, a nicoletti assay revealed that when H9c2 cells were exposed to 10% O_2 for 48 hours, there is a 44% increase in the proliferative index (the proportion of cells in the G_2 phase/G_1 phase), indicating a hypoxia-induced increase in mitosis. However, when we added misoprostol to hypoxic cells, the proliferative index was reduced by nearly 15%, representing a partial rescue of the proliferative phenotype (Fig 1, H).

Hypoxia and misoprostol promote cardiomyocyte hypertrophy

Given the central role of nuclear calcium in the regulation of cardiac transcription factors, we first assessed nuclear calcium content. Using H9c2's, in combination with a nuclear targeted calcium biosensor (NLS-GECO) (46), we observed that 10% O_2 for 48 hours does not alter nuclear calcium content, but misoprostol treatment in the presence of hypoxia, increased nuclear calcium by more than 66% (Fig. 2, A & B).

Next, we looked at how this calcium signal may directly impact the localization of the calcineurin target, NFATc3. Using H9c2 cells, we expressed myc-NFATc3 and exposed to cells to hypoxia, with and without misoprostol. Consistent with our nuclear calcium data, misoprostol alone had little effect on the accumulation of NFATc3 in the nucleus, but the combination of hypoxia and misoprostol resulted in a more than 5-fold increase in nuclear NFATc3 accumulation (Fig. 2, C & D). We also looked at the localization of the NFAT interacting partner, NF-κB (27). Consistent with what we have shown previously (13),

misoprostol treatment alone increased PVNC nuclear NF-κB by more than 4.6-fold, but the combination of hypoxia and misoprostol resulted in a 5.95-fold increase, compared to normoxic control (Fig. 2, E & F). We confirmed the NFATc3 observation endogenously by fractionation in H9c2 cells that were exposed to 10% O_2 with and without misoprostol for 48 hours. Here we observed that hypoxia and misoprostol shifts NFATc3 away from the cytosol and into the nucleus (Fig 2, G).

We also assessed the impact of hypoxia and misoprostol treatment on neonatal cardiac gene expression. Using western blot analysis of PVNC's we first observed that hypoxia increased the expression MEF2C, the MEF2 family member associated with fetal cardiomyocyte proliferation, while MEF2A expression remained unchanged from control. Furthermore, the induction of MEF2C observed following hypoxia was absent when combined with misoprostol treatment; however, MEF2A expression was sustained (Fig. 2, H). We next evaluated the MEF2C target-gene, myocardin, which in the PND10 heart was unchanged by hypoxia, but was significantly reduced with the combination of hypoxia and misoprostol (Fig. 2, I), suggesting that the combination of hypoxia and prostaglandin signaling is required for myocardin repression. Finally, we observed that hypoxia increased proliferative BMP10 expression by 58.5% , which was significantly reduced with the addition of misoprostol (Fig. 2, J).

sNip opposes hypoxia-induced neonatal cardiomyocyte proliferation

Previously, we demonstrated that misoprostol treatment in HCT-116 cells leads to nuclear retention of the p65 subunit of NF-κB (13). Moreover, when combined with HIF1α activation, this combination of transcription factors was sufficient to drive Bnip3 splicing in favour of sNip expression (13). Thus, we performed western blot analysis on neonatal hearts and H9c2 cells exposed to hypoxia and/or misoprostol treatment to evaluate sNip expression. We observed that in both PND10 hearts and H9c2 cells, the combination of hypoxia and misoprostol increases the expression of the small Bnip3 isoform, sNip (Fig. 3, A & B).

In order to explore the role of sNip as a mechanism for misoprostol-induced blockade of cell cycle reentry, we performed a series of knock-down experiments using an siRNA targeting sNip. When H9c2 cells were exposed to hypoxia, we observed a more than 3.8-fold increase in the number of proliferative

nuclei, compared to normoxia-treated control cells. When these cells were treated with misoprostol to induce sNip expression, proliferation was reduced by 79.7%, back to control levels. However, when cells were transfected with an siRNA targeting sNip, misoprostol treatment was no longer able to reduce cell proliferation (Fig. 3, C & D). Next, we evaluated whether ectopic sNip expression was able to phenocopy the effects of misoprostol in PVNC's. To do this, cells were transduced with sNip lentivirus, and then exposed to 10% O_2 for 48 hours. We observed a nearly 6-fold increase in proliferative nuclei with hypoxia exposure, that was completely abrogated with sNip expression, consistent with our misoprostol findings in Figure 3E & F.

To further confirm the cell cycle suppressive properties of sNip at the cell population level, we performed nicoletti assays using H9c2 cells that were transfected with sNip or an empty vector control. We observed that cells expressing sNip displayed a 14.5% reduction in their proliferative index compared to control, shifting the population further into the G_1 classification rather than G_2 (Fig. 3, G).

sNip promotes cardiomyocyte hypertrophy in an NFATc3 dependent manner

Next, we determined the impact of sNip expression on the calcium-dependent gene expression alterations we observed with misoprostol treatment in hypoxic cardiomyocytes. First, we utilized the nuclear calcium biosensor NLS-GECO in H9c2 cells expressing sNip or empty vector, and exposed to normoxia or 10% O_2 for 48 hours. We observed that both sNip on its own and in combination with hypoxia were sufficient to induced calcium accumulation in the nucleus (Fig. 4, A & B).

Given that the endoplasmic/sarcoplasmic reticulum (ER/SR) contains a large pool of intracellular calcium and is continuous with the outer membrane of the perinuclear envelope, we sought to determine if the ER/SR was the source of cellular calcium that was accumulating in the nuclear under the influence of sNip. We used the ER targeted calcium biosensor (ER-LAR-GECO), described previously, to assess ER/SR calcium content. Interestingly, when expressed in H9c2 cells sNip reduced ER calcium content by 58.8% compared to control (Fig. 4, C & D). In a parallel series of experiments, sNip also enhanced nuclear calcium content; however, when cells were treated with the IP_3 receptor inhibitor, 2-APB (47), nuclear calcium was restored back to control levels (Fig. 4, E & F). Furthermore, blockade of the ryanodine receptor with

dantrolene was also able to block sNip-induced nuclear calcium accumulation, but the magnitude of this blockade was less than for 2APB (Fig.4, G).

Finally, we expressed sNip in H9c2 cells to evaluate its direct effect on transcription factor localization and gene expression. Using subcellular fractionation to separate components of the cytosolic compartment from components of the nuclear compartment, we observed that sNip increased the nuclear localization of NFATc3, compared to cells expressing an empty vector control (Fig. 4, H). We confirmed this observation using immunofluorescence, where sNip expression in H9c2 cells resulted in a 2.96-fold increase in the nuclear localization of NFATc3 (Fig. 4, I & J). In addition, sNip transduction in PVNC's reduced the expression of myocardin (43%), BMP10 (66%) and MEF2C (55%), and increased the expression of the NF-κB targeting gene BMP2 by 794% (Fig. 4, K), determined by real-time PCR.

Discussion:

Hypoxia exposure in the neonatal heart is considered detrimental to cardiac development, increasing the risk of pediatric heart failure, and lifelong cardiovascular abnormalities. However, recently it has been observed that the underlying cause may involve aberrant cardiomyocyte proliferation. In this report, we show that hypoxia drives cardiomyocyte proliferation, concurrent with activation of a MEF2C and BMP10 pathway. We also provide evidence that PGE1 signalling through misoprostol treatment is able to activate a secondary and opposing pathway, enhancing Bnip3 splicing to produce sNip. This alternative splicing of the Bnip3 protein results in nuclear calcium accumulation and calcium-induced gene expression, promoting cardiomyocyte maturation and attenuating hypoxia-induced proliferation.

The results in the present study expand on previous reports that early life hypoxia exposure is sufficient to drive neonatal cardiomyocyte proliferation. These previous studies have mainly focused on the conditions required for, and the regenerative capacity of, hypoxia-induced cardiomyocyte proliferation (20, 32, 34). Interestingly, maintaining a capacity for proliferation after birth appears to depend on the metabolic status of the cardiomyocyte, where the switch from glycolysis to oxidative phosphorylation and the resultant accumulation of cytotoxic free radicals is thought to result in cardiomyocyte senescence (37). Moreover,

recent evidence further suggests that preventing this metabolic shift is key to maintaining c-kit^{+} cardiac progenitor cells in culture (21).

While the literature to date has primarily focused on the role of cellular metabolism, our data provides insight into the underlying hypoxia-driven mechanisms promoting neonatal cardiomyocyte proliferation. In this report, we confirm that expression of MEF2C is hypoxia inducible, and that this may be a key cardiac-enriched initiator of a hypoxia-induced cardiomyocyte proliferation (2, 23). Furthermore, evidence supports the existence of a feed-forward loop promoting proliferation that hinges on MEF2C-dependent activation of myocardin and downstream BMP10 expression. This proposed mechanism builds on the observation that myocardin and MEF2C closely regulate each other, and that loss of myocardin prevents MEF2C expression (7, 18). Importantly, myocardin also directly regulates BMP10 expression, and loss of the myocardin/BMP10 signalling pathway negatively impacts cardiomyocyte proliferation (18). Furthermore, BMP10 also appears to be required for maintaining MEF2C expression and preventing myocyte maturation, which may function to propagate proliferation and alter the structure of the developing heart heart (4).

Many previous studies have assessed methods to extend the period of post-natal cardiomyocyte proliferation (20, 33, 35, 37). However, in the context of early life hypoxic/cyanotic events there may be direct benefits to pharmacologically targeting cardiomyocyte proliferation. Our data demonstrates that activation of PGE1 signalling through misoprostol can inhibit the MEF2C-Myocardin-BMP10 pathway. Furthermore, we show that the protective effects of misoprostol are dependent on the expression of the small Bnip3 isoform, sNip. Previous work from our group, and others, have demonstrated that while sNip is hypoxia-inducible, NF-κB activity is crucial for its expression in cardiomyocytes (13, 14). Interestingly, much of sNip's opposition to cardiomyocyte proliferation appears to based on its ability to promote the transfer of calcium from the SR/ER to the nucleus. This builds on our recent findings that sNip possesses a C-terminal ER retention signal, and that unlike full-length Bnip3, sNip expression in cardiomyocytes functions to sustained nuclear calcium accumulation (13). Nuclear calcium signaling is known to activate calcium-calmodulin dependent transcriptional regulators, such as the calcineurin and NFAT pathway (6,

29, 30, 42). Our findings demonstrate that misoprostol treatment leads to the nuclear accumulation of both NF-κB and NFATc3, through distinct pathways, to promote cardiomyocyte growth and maturation over proliferation. This observation is consistent with previous work demonstrating that NFAT and NF-κB are considerably less efficient at producing a hypertrophic response alone than when the two are expressed together (27). Additionally, our data suggests that this combination of transcription factors may be responsible for BMP2 expression in the neonatal heart, which likely promotes maturation and may oppose proliferative BMP10 signaling. Supporting this notion, the BMP2 promoter region has been shown to possess an NF-κB binding site, suggesting that sNip may activate the cooperation between NFAT and NF-κB to induced BMP2 expression in the neonatal heart (12, 15).

Collectively, our data demonstrates that the activation of PGE1 signalling through misoprostol treatment is sufficient to mitigate hypoxia-induced proliferation in neonatal cardiomyocytes through a mechanism involving alternative splicing of Bnip3 and activation of NFAT and NF-κB. Moreover, our findings suggest that pharmacological fine-tuning of the underlying molecular mechanisms that control hypoxia-induced cardiomyocyte proliferation may represent a novel strategy to prevent pediatric cardiac dysfunction and reduce the risk of early-life heart failure.

Acknowledgments:

This work was supported by a Natural Sciences and Engineering Research Council (NSERC) Canada Discovery Grant and a Heart and Stroke Foundation of Canada Grant-in-Aid to J.W.G. T.L.I. is funded through the SFRG and UCRP programs from the University of Manitoba. J.W.G. and A.R.W. are members of the DEVOTION Research Cluster. M.D.M. and J.T.F. are supported by studentships from the Children's Hospital Foundation of Manitoba and Research Manitoba, M.D.M. received support from the DEVOTION research cluster.

Conflicts:

None.

Author Contributions:

MDM and JWG conceived and coordinated the study. MDM and JWG wrote the paper. MDM designed and conducted most of the experiments. MDM was also responsible for data analysis and presentation. JTF conducted flow cytometry and fractionation experiments. DC designed and conducted the qRT-PCR experiments. TLI designed and conducted the in vivo hypoxia experiments. JWG, TLI and ARW were responsible for funding acquisition. All authors reviewed the results, edited, and approved the final version of the manuscript.

References:

1. **Azad MB**, **Chen Y**, **Henson ES**, **Cizeau J**, **McMillan-Ward E**, **Israels SJ**, **Gibson SB**. Hypoxia induces autophagic cell death in apoptosis-competent cells through a mechanism involving BNIP3. *Autophagy* 4: 195–204, 2008.
2. **Bohuslavova R**, **Skvorova L**, **Sedmera D**, **Semenza GL**, **Pavlinkova G**. Increased susceptibility of HIF-1α heterozygous-null mice to cardiovascular malformations associated with maternal diabetes. *J Mol Cell Cardiol* 60: 129–141, 2013.
3. **Carr H**, **Cnattingius S**, **Granath F**, **Ludvigsson JF**, **Edstedt Bonamy AK**. Preterm Birth and Risk of Heart Failure Up to Early Adulthood. *J Am Coll Cardiol* 69: 2634–2642, 2017.
4. **Chen H**, **Shi S**, **Acosta L**, **Li W**, **Lu W**, **Bao S**, **Chen Z**, **Yang Z**, **Schneider MD**, **Chien KR**, **Conway SJ**, **Yoder MC**, **Haneline LS**, **Franco D**, **Shou W**. BMP10 is essential for maintaining cardiac growth during murine cardiogenesis. *Development* 131: 2219–2231, 2004.
5. **Cox DJ**, **Edwards AD**, **Hajnal JV**, **Durighel G**, **Price AN**, **Broadhouse KM**, **Groves AM**, **Finnemore AE**. Cardiovascular magnetic resonance of cardiac function and myocardial mass in preterm infants: a preliminary study of the impact of patent ductus arteriosus. *J Cardiovasc Magn Reson* 16: 1–9, 2014.
6. **Crabtree GR**, **Olson EN**. NFAT Signaling. *Cell* 109: S67–S79, 2002.
7. **Creemers EE**, **Sutherland LB**, **McAnally J**, **Richardson JA**, **Olson EN**. Myocardin is a direct transcriptional target of Mef2, Tead and Foxo proteins during cardiovascular development. *Development* 133: 4245–4256, 2006.
8. **de la Pompa JL**, **Epstein JA**. Coordinating Tissue Interactions: Notch Signaling in Cardiac Development and Disease. *Dev Cell* 22: 244–254, 2012.
9. **Desjardins C**, **Naya F**. The Function of the MEF2 Family of Transcription Factors in Cardiac Development, Cardiogenomics, and Direct Reprogramming. *J Cardiovasc Dev Dis* 3: 26–26, 2016.
10. **Desjardins CA**, **Naya FJ**. Antagonistic regulation of cell-cycle and differentiation gene programs in neonatal cardiomyocytes by homologous MEF2 transcription factors. *J Biol Chem* 292: 10613–10629, 2017.
11. **Diehl-Jones W**, **Archibald A**, **Gordon JW**, **Mughal W**, **Hossain Z**, **Friel JK**. Human Milk Fortification Increases Bnip3 Expression Associated With Intestinal Cell Death In Vitro. *J Pediatr Gastroenterol Nutr* 61: 583–590, 2015.
12. **Feng JQ**, **Xing L**, **Zhang J-H**, **Zhao M**, **Horn D**, **Chan J**, **Boyce BF**, **Harris SE**, **Mundy GR**, **Chen D**. NF-κB Specifically Activates BMP-2 Gene Expression in Growth Plate Chondrocytes in Vivo and in a Chondrocyte Cell Line in Vitro. *J Biol Chem* 278: 29130–29135, 2003.
13. **Field JT**, **Martens MD**, **Mughal W**, **Hai Y**, **Chapman D**, **Hatch GM**, **Ivanco TL**, **Diehl-Jones W**, **Gordon JW**. Misoprostol regulates Bnip3 repression and alternative splicing to control cellular calcium homeostasis during hypoxic stress. *Cell Death Discov* 4: 98–98, 2018.

14. **Gang H**, **Hai Y**, **Dhingra R**, **Gordon JW**, **Yurkova N**, **Aviv Y**, **Li H**, **Aguilar F**, **Marshall A**, **Leygue E**, **Kirshenbaum LA**. A novel hypoxia-inducible spliced variant of mitochondrial death gene Bnip3 promotes survival of ventricular myocytes. *Circ Res* 108: 1084–1092, 2011.
15. **Gordon JW**, **Shaw JA**, **Kirshenbaum LA**. Multiple facets of NF-kB in the heart: To be or not to NF-kB. *Circ Res* 108: 1122–1132, 2011.
16. **Gustafsson ÅB**. Bnip3 as a dual regulator of mitochondrial turnover and cell death in the myocardium. *Pediatr Cardiol* 32: 267–274, 2011.
17. **Hanna RA**, **Quinsay MN**, **Orogo AM**, **Giang K**, **Rikka S**, **Gustafsson ÅB**. Microtubule-associated protein 1 light chain 3 (LC3) interacts with Bnip3 protein to selectively remove endoplasmic reticulum and mitochondria via autophagy. *J Biol Chem* 287: 19094–19104, 2012.
18. **Huang J**, **Elicker J**, **Bowens N**, **Liu X**, **Cheng L**, **Cappola TP**, **Zhu X**, **Parmacek MS**. Myocardin regulates BMP10 expression and is required for heart development. *J Clin Invest* 122: 3678–3691, 2012.
19. **Kim Y**, **Phan D**, **van Rooij E**, **Wang D-Z**, **McAnally J**, **Qi X**, **Richardson JA**, **Hill JA**, **Bassel-Duby R**, **Olson EN**. The MEF2D transcription factor mediates stress-dependent cardiac remodeling in mice. *J Clin Invest* 118: 124–132, 2008.
20. **Kimura W**, **Xiao F**, **Canseco DC**, **Muralidhar S**, **Thet S**, **Zhang HM**, **Abderrahman Y**, **Chen R**, **Garcia JA**, **Shelton JM**, **Richardson JA**, **Ashour AM**, **Asaithamby A**, **Liang H**, **Xing C**, **Lu Z**, **Zhang CC**, **Sadek HA**. Hypoxia fate mapping identifies cycling cardiomyocytes in the adult heart. *Nature* 523: 226–230, 2015.
21. **Korski KI**, **Kubli DA**, **Wang BJ**, **Khalafalla FG**, **Monsanto MM**, **Firouzi F**, **Echeagaray OH**, **Kim T**, **Adamson RM**, **Dembitsky WP**, **Gustafsson ÅB**, **Sussman MA**. Hypoxia Prevents Mitochondrial Dysfunction and Senescence in Human c-Kit + Cardiac Progenitor Cells: Hypoxia Blunts Senescence of Cardiac Stem Cells. *STEM CELLS* 37: 555–567, 2019.
22. **Kothari S**, **Cizeau J**, **McMillan-Ward E**, **Israels SJ**, **Bailes M**, **Ens K**, **Kirshenbaum LA**, **Gibson SB**. BNIP3 plays a role in hypoxic cell death in human epithelial cells that is inhibited by growth factors EGF and IGF. *Oncogene* 22: 4734–4744, 2003.
23. **Krishnan J**, **Ahuja P**, **Bodenmann S**, **Knapik D**, **Perriard E**, **Krek W**, **Perriard J-C**. Essential Role of Developmentally Activated Hypoxia-Inducible Factor 1α for Cardiac Morphogenesis and Function. *Circ Res* 103: 1139–1146, 2008.
24. **Kubli DA**, **Ycaza JE**, **Gustafsson ÅB**. Bnip3 mediates mitochondrial dysfunction and cell death through Bax and Bak. *Biochem J* 405: 407–415, 2007.
25. **Lewandowski AJ**, **Augustine D**, **Lamata P**, **Davis EF**, **Lazdam M**, **Francis J**, **McCormick K**, **Wilkinson AR**, **Singhal A**, **Lucas A**, **Smith NP**, **Neubauer S**, **Leeson P**. Preterm Heart in Adult Life. *Circulation* 127: 197–206, 2012.
26. **Lin Q**, **Schwarz J**, **Bucana C**, **Olson EN**. Control of Mouse Cardiac Morphogenesis and Myogenesis by Transcription Factor MEF2C. *Science* 276: 1404–1407, 1997.
27. **Liu Q**, **Chen Y**, **Auger-Messier M**, **Molkentin JD**. Interaction between NFκB and NFAT coordinates cardiac hypertrophy and pathological remodeling. *Circ Res* 110: 1077–1086, 2012.
28. **Moghadam AR**, **da Silva Rosa SC**, **Samiei E**, **Alizadeh J**, **Field J**, **Kawalec P**, **Thliveris J**, **Akbari M**, **Ghavami S**, **Gordon JW**. Autophagy modulates temozolomide-induced cell death in alveolar Rhabdomyosarcoma cells. *Cell Death Discov* 4: 52, 2018.
29. **Molkentin J**. Calcineurin-NFAT signaling regulates the cardiac hypertrophic response in coordination with the MAPKs. *Cardiovasc Res* 63: 467–475, 2004.
30. **Molkentin JD**, **Lu J-R**, **Antos CL**, **Markham B**, **Richardson J**, **Robbins J**, **Grant SR**, **Olson EN**. A Calcineurin-Dependent Transcriptional Pathway for Cardiac Hypertrophy. *Cell* 93: 215–228, 1998.
31. **Mughal W**, **Martens M**, **Field J**, **Chapman D**, **Huang J**, **Rattan S**, **Hai Y**, **Cheung KG**, **Kereliuk S**, **West AR**, **Cole LK**, **Hatch GM**, **Diehl-Jones W**, **Keijzer R**, **Dolinsky VW**, **Dixon IM**, **Parmacek MS**, **Gordon JW**. Myocardin regulates mitochondrial calcium homeostasis and prevents permeability transition. *Cell Death Differ* 25: 1732–1748, 2018.

32. **Mughal W**, **Nguyen L**, **Pustylnik S**, **da Silva Rosa SC**, **Piotrowski S**, **Chapman D**, **Du M**, **Alli NS**, **Grigull J**, **Halayko AJ**, **Aliani M**, **Topham MK**, **Epand RM**, **Hatch GM**, **Pereira TJ**, **Kereliuk S**, **McDermott JC**, **Rampitsch C**, **Dolinsky VW**, **Gordon JW**. A conserved MADS-box phosphorylation motif regulates differentiation and mitochondrial function in skeletal, cardiac, and smooth muscle cells. *Cell Death Dis* 6: e1944–e1944, 2015.
33. **Nakada Y**, **Canseco DC**, **Thet S**, **Abdisalaam S**, **Asaithamby A**, **Santos CX**, **Shah AM**, **Zhang H**, **Faber JE**, **Kinter MT**, **Szweda LI**, **Xing C**, **Hu Z**, **Deberardinis RJ**, **Schiattarella G**, **Hill JA**, **Oz O**, **Lu Z**, **Zhang CC**, **Kimura W**, **Sadek HA**. Hypoxia induces heart regeneration in adult mice. *Nature* 541: 222–227, 2017.
34. **Naya FJ**, **Black BL**, **Wu H**, **Bassel-Duby R**, **Richardson JA**, **Hill JA**, **Olson EN**. Mitochondrial deficiency and cardiac sudden death in mice lacking the MEF2A transcription factor. *Nat Med* 8: 1303–1309, 2002.
35. **Porrello ER**, **Mahmoud AI**, **Simpson E**, **Hill JA**, **Richardson JA**, **Olson EN**, **Sadek HA**. Transient Regenerative Potential of the Neonatal Mouse Heart. 2011.
36. **Posod A**, **Odri Komazec I**, **Kager K**, **Pupp Peglow U**, **Griesmaier E**, **Schermer E**, **Würtinger P**, **Baumgartner D**, **Kiechl-Kohlendorfer U**. Former Very Preterm Infants Show an Unfavorable Cardiovascular Risk Profile at a Preschool Age. *PLOS ONE* 11: e0168162, 2016.
37. **Puente BN**, **Kimura W**, **Muralidhar SA**, **Moon J**, **Amatruda JF**, **Phelps KL**, **Grinsfelder D**, **Rothermel BA**, **Chen R**, **Garcia JA**, **Santos CX**, **Thet S**, **Mori E**, **Kinter MT**, **Rindler PM**, **Zacchigna S**, **Mukherjee S**, **Chen DJ**, **Mahmoud AI**, **Giacca M**, **Rabinovitch PS**, **Aroumougame A**, **Shah AM**, **Szweda LI**, **Sadek HA**. The oxygen-rich postnatal environment induces cardiomyocyte cell-cycle arrest through DNA damage response. *Cell* 157: 565–579, 2014.
38. **Quinsay MN**, **Lee Y**, **Rikka S**, **Sayen MR**, **Molkentin JD**, **Gottlieb RA**, **Gustafsson ÅB**. Bnip3 mediates permeabilization of mitochondria and release of cytochrome c via a novel mechanism. *J Mol Cell Cardiol* 48: 1146–1156, 2010.
39. **Quinsay MN**, **Thomas RL**, **Lee Y**, **Gustafsson ÅB**. Bnip3-mediated mitochondrial autophagy is independent of the mitochondrial permeability transition pore. *Autophagy* 6: 855–862, 2010.
40. **dos Remedios CG**, **Colan S**, **Savla J**, **Park S**, **Kühn B**, **Bersell K**, **Graham D**, **Walsh S**, **Mollova M**, **Silberstein LE**, **Das LT**. Cardiomyocyte proliferation contributes to heart growth in young humans. *Proc Natl Acad Sci* 110: 1446–1451, 2013.
41. **Riccardi C**, **Nicoletti I**. Analysis of apoptosis by propidium iodide staining and flow cytometry. *Nat Protoc* 1: 1458–1461, 2006.
42. **Wilkins BJ**, **Molkentin JD**. Calcineurin and cardiac hypertrophy: Where have we been? Where are we going? *J Physiol* 541: 1–8, 2002.
43. **Wu H**, **Naya FJ**, **McKinsey TA**, **Mercer B**, **Shelton JM**, **Chin ER**, **Simard AR**, **Michel RN**, **Bassel-Duby R**, **Olson EN**, **Williams RS**. MEF2 responds to multiple calcium-regulated signals in the control of skeletal muscle fiber type. *EMBO J* 19: 1963–1973, 2000.
44. **Wu H**, **Rothermel B**, **Kanatous S**, **Rosenberg P**, **Naya FJ**, **Shelton JM**, **Hutcheson KA**, **DiMaio JM**, **Olson EN**, **Bassel-Duby R**, **Williams RS**. Activation of MEF2 by muscle activity is mediated through a calcineurin-dependent pathway. *EMBO J* 20: 6414–6423, 2001.
45. **Wu J**, **Liu L**, **Matsuda T**, **Zhao Y**, **Rebane A**, **Drobizhev M**, **Chang YF**, **Araki S**, **Arai Y**, **March K**, **Hughes TE**, **Sagou K**, **Miyata T**, **Nagai T**, **Li WH**, **Campbell RE**. Improved orange and red Ca2+ indicators and photophysical considerations for optogenetic applications. *ACS Chem Neurosci* 4: 963–972, 2013.
46. **Wu J**, **Prole DL**, **Shen Y**, **Lin Z**, **Gnanasekaran A**, **Liu Y**, **Chen L**, **Zhou H**, **Chen SRW**, **Usachev YM**, **Taylor CW**, **Campbell RE**. Red fluorescent genetically encoded Ca 2+ indicators for use in mitochondria and endoplasmic reticulum. *Biochem J* 464: 13–22, 2014.
47. **Wu X**, **Zhang T**, **Bossuyt J**, **Li X**, **McKinsey TA**, **Dedman JR**, **Olson EN**, **Chen J**, **Brown JH**, **Bers DM**. Local InsP3-dependent perinuclear Ca2+ signaling in cardiac myocyte excitation-transcription coupling. *J Clin Invest* 116: 675–682, 2006.
48. **Zeglinski MR**, **Moghadam AR**, **Ande SR**, **Sheikholeslami K**, **Mokarram P**, **Sepehri Z**, **Rokni**

H, **Mohtaram NK**, **Poorebrahim M**, **Masoom A**, **Toback M**, **Sareen N**, **Saravanan S**, **Jassal DS**, **Hashemi M**, **Marzban H**, **Schaafsma D**, **Singal P**, **Wigle JT**, **Czubryt MP**, **Akbari M**, **Dixon IMC**, **Ghavami S**, **Gordon JW**, **Dhingra S**. Myocardial Cell Signaling During the Transition to Heart Failure: Cellular Signaling and Therapeutic Approaches. *Compr Physiol* 9: 75–125, 2018.

Figure Legends:

Figure 1. Misoprostol opposes hypoxia-induced neonatal cardiomyocyte proliferation. (A) Neonatal heart weights (in grams) for PND10 rat pups exposed to hypoxia (10% O_2) ± 10 μg/kg misoprostol for 5 days (n ≥ 3 animals/condition). **(B)** Masson's Trichrome and Hematoxylin and Eosin staining in the left ventricle of the PND10 heart treated as in (A). **(C)** Quantification of left ventricular nuclei number in the PND10 rat heart as treated in (A) (n=3 animals/condition, with 10 fields/animal). **(D)** Densitometry for Cyclin-D1 expression (relative to β-Tubulin) in protein extracts from the whole PND10 heart treated as in (A) (n=2). **(E)** Immunoblot for Cyclin-D1 and p57(KP39) in protein extracts from primary ventricular neonatal cardiomyocytes (PVNC's) treated with 10 μM misoprostol (Miso) ± 10% O_2 (HPX) for 48 hours. **(F)** PVNC's treated as in (E), and stained with Tag-it Violet (blue) and calcein-AM (green) and imaged by standard fluorescence microscopy. **(G)** Quantification of Tag-it Violet positive cells in (F), where the number of blue cells is represented as a percentage (%) of the total number of (green) cells in 10 random fields. **(H)** DNA Histograms of H9c2 cells treated as in (E), where G_1 indicates cells that are 2N and G_2 indicates cells that are 4N and G_2/G_1 ratio indicates the proliferative index. Data are represented as mean ± S.E.M. **P*<0.05 compared with control, while ***P*<0.05 compared with hypoxia treatment, determined by 1-way ANOVA.

Figure 2. Hypoxia and misoprostol work together to promote cardiomyocyte hypertrophy. (A) H9c2 cells treated with 10 μM misoprostol (Miso) ± 10% O_2 (HPX) for 48 hours. NLS-R-GECO (red) was used to indicate nuclear calcium content in all conditions. Cells were stained with hoechst (blue) and imaged by standard fluorescence microscopy. **(B)** Quantification of cells in (A), where red fluorescent signal was normalized to cell area and quantified in 10 random fields. **(C)** H9c2 cells treated as in (A) and Myc-NFATc3 was transfected into each condition. Cells were fixed, stained with hoechst (blue), and probed for Myc (green) expression. Cells were then imaged by standard fluorescence microscopy. **(D)** Quantification

of cells in (C), where the number of cells with nuclear Myc-NFATc3, is presented as a percentage of the number of cells/field in 5 random fields. **(E)** PVNC's treated as in (A), Cells were fixed, stained with hoechst (blue), and probed for nuclear factor kappa-B (Anti-NF-κB, green) expression. Cells were then imaged by standard fluorescence microscopy. **(F)** Quantification of cells in (E), where the number of cells with nuclear NF-κB, is presented as a percentage of the number of cells/field in 10 random fields. **(G)** H9c2 cells were treated as in (A), Protein extracts were subjected to nuclear/cytosolic fractionation and were immunoblotted, as indicated. **(H)** Immunoblot for MEF2C and MEF2A in protein extracts from PVCs treated as in (A). **(I)** Densitometry for myocardin expression in in protein extracts from whole PND10 hearts exposed to hypoxia (10% O_2) ± 10 μg/kg misoprostol for 5 days (n ≥ 3 animals/condition). **(J)** PVNC's treated as in (A). RNA was isolated and qRT-PCR was performed for BMP-10 expression. Data are represented as mean ± S.E.M. **P*<0.05 compared with control, while ***P*<0.05 compared with hypoxia treatment, determined by 1-way ANOVA.

Figure 3. sNip opposes hypoxia-induced neonatal cardiomyocyte proliferation. (A) Immunoblot for sNip expression in protein extracts from whole PND10 hearts exposed to hypoxia (10% O_2) ± 10 μg/kg misoprostol for 5 days. **(B)** Immunoblot for sNip expression in H9c2 protein extracts treated with 10 μM misoprostol (Miso) ± 10% O_2 (HPX) for 48 hours. **(C)** H9c2 cells treated as in (B), transfected with scrambled control si-RNA or si-sNip, and stained with Tag-it Violet (blue) and calcein-AM (green) and imaged by standard fluorescence microscopy. **(D)** Quantification of Tag-it Violet positive cells in (C), where the number of blue cells is represented as a percentage (%) of the total number of (green) cells in 10 random fields. **(E)** PVNC's treated with pLenti-HA-sNip ± 10% O_2 (HPX) for 48 hours and stained with Tag-it Violet (blue) and calcein-AM (green) and imaged by standard fluorescence microscopy. **(F)** Quantification of Tag-it Violet positive cells in (E), where the number of blue cells is represented as a percentage (%) of the total number of (green) cells in 10 random fields. **(G)** DNA Histograms of H9c2 cells transfected with empty vector control or HA-sNip, where G_1 indicates cells that are 2N and G_2 indicates cells that are 4N and G_2/G_1 ratio indicates the proliferative index. Data are represented as mean ± S.E.M.

*P<0.05 compared with control, while **P<0.05 compared with hypoxia treatment, determined by 1-way ANOVA.

Figure 4. sNip promotes cardiomyocyte hypertrophy in an NFATc3-dependent manner. (A) H9c2 cells transfected with sNip or empty vector control ± 10% O_2 (HPX) for 48 hours. NLS-R-GECO (red) was used to indicate nuclear calcium content in all conditions. Cells were stained with hoechst (blue) and imaged by standard fluorescence microscopy. **(B)** Quantification of cells in (A), where red fluorescent signal was normalized to cell area and quantified in 10 random fields. **(C)** H9c2 cells transfected with sNip or empty vector control. ER-LAR-GECO (red) was used to indicate endoplasmic reticulum calcium content in all conditions. Cells were stained with hoechst (blue) and imaged by standard fluorescence microscopy. **(D)** Quantification of cells in (C), Red fluorescent signal was normalized to cell area and quantified in 10 random fields. **(E)** H9c2 cells transfected with sNip or empty vector control ± 2 μM 2-APB for 16 hours. NLS-R-GECO (red) was used to indicate nuclear calcium content in all conditions. Cells were stained with hoechst (blue) and imaged by standard fluorescence microscopy. **(F)** Quantification of cells in (E), where red fluorescent signal was normalized to cell area and quantified in 10 random fields. **(G)** Quantification of H9c2 cells transfected with sNip or empty vector control ± 10 μM Dantrolene (DAN) for 16 hours, NLS-R-GECO (red) was used to indicate nuclear calcium content in all conditions. Red fluorescent signal was normalized to cell area and quantified in 10 random fields. **(H)** H9c2 cells treated as in (C), Protein extracts were subjected to nuclear/cytosolic fractionation and were immunoblotted, as indicated. **(I)** H9c2 cells treated as in (C). CMV-dsRed and Myc-NFATc3 were included in all conditions to indicate transfected cells. Cells were fixed, stained with hoechst (blue), and probed for Myc (green) expression. Cells were then imaged by standard fluorescence microscopy. **(J)** Quantification of cells in (I), where the number of cells with nuclear Myc-NFATc3, is presented as a percentage of the number of cells/field in 5 random fields. **(K)** mRNA expression in PVNC's transduced with scrambled control virus or pLenti-sNip. RNA was isolated and qRT-PCR was performed for Myocardin (MYOCD), BMP-10, BMP-2, MEF2C and MEF2A expression. Data are represented as mean ± S.E.M. *P<0.05 compared with control, while **P<0.05 compared with hypoxia treatment, determined by 1-way ANOVA.

Figure 1

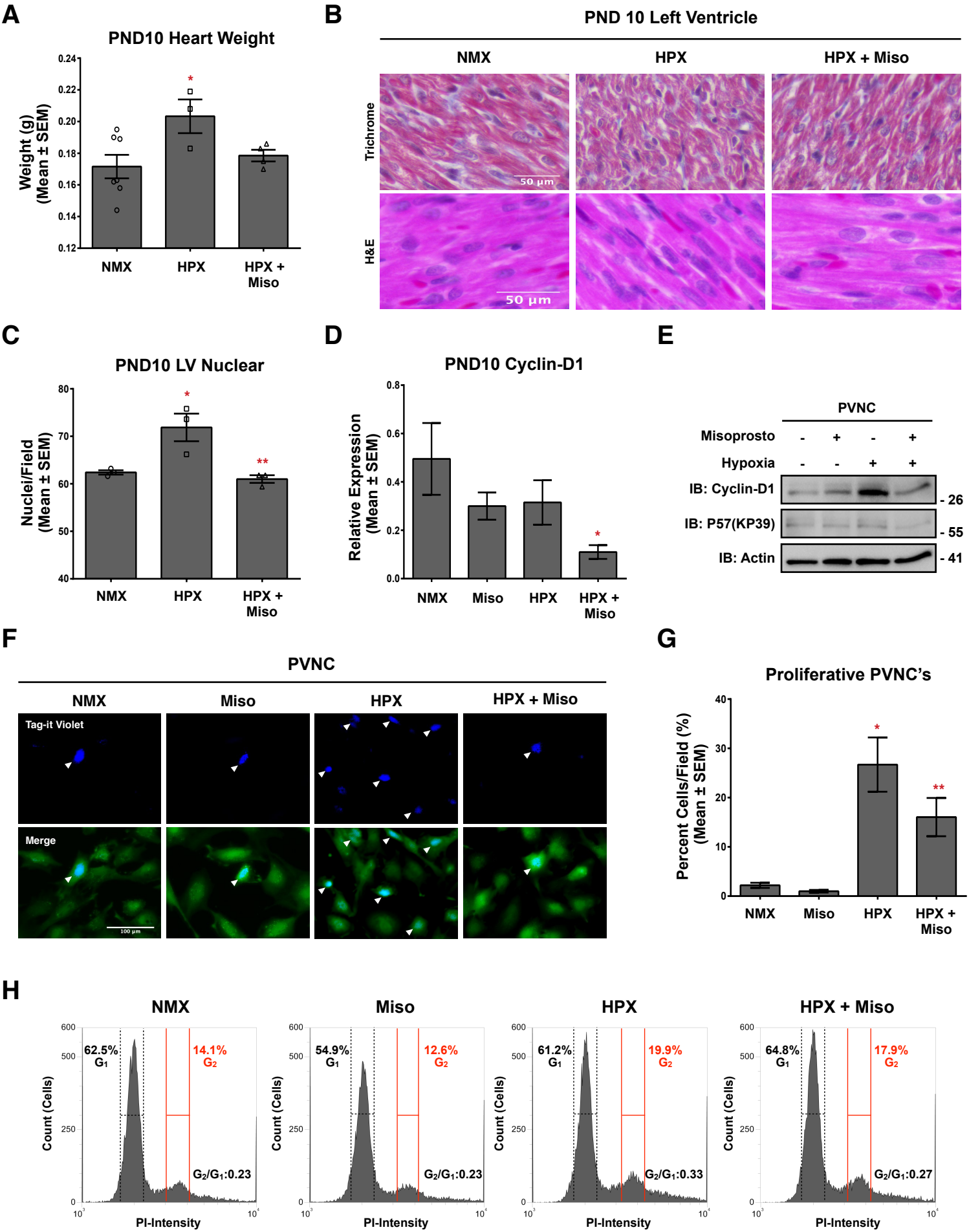

Figure 2

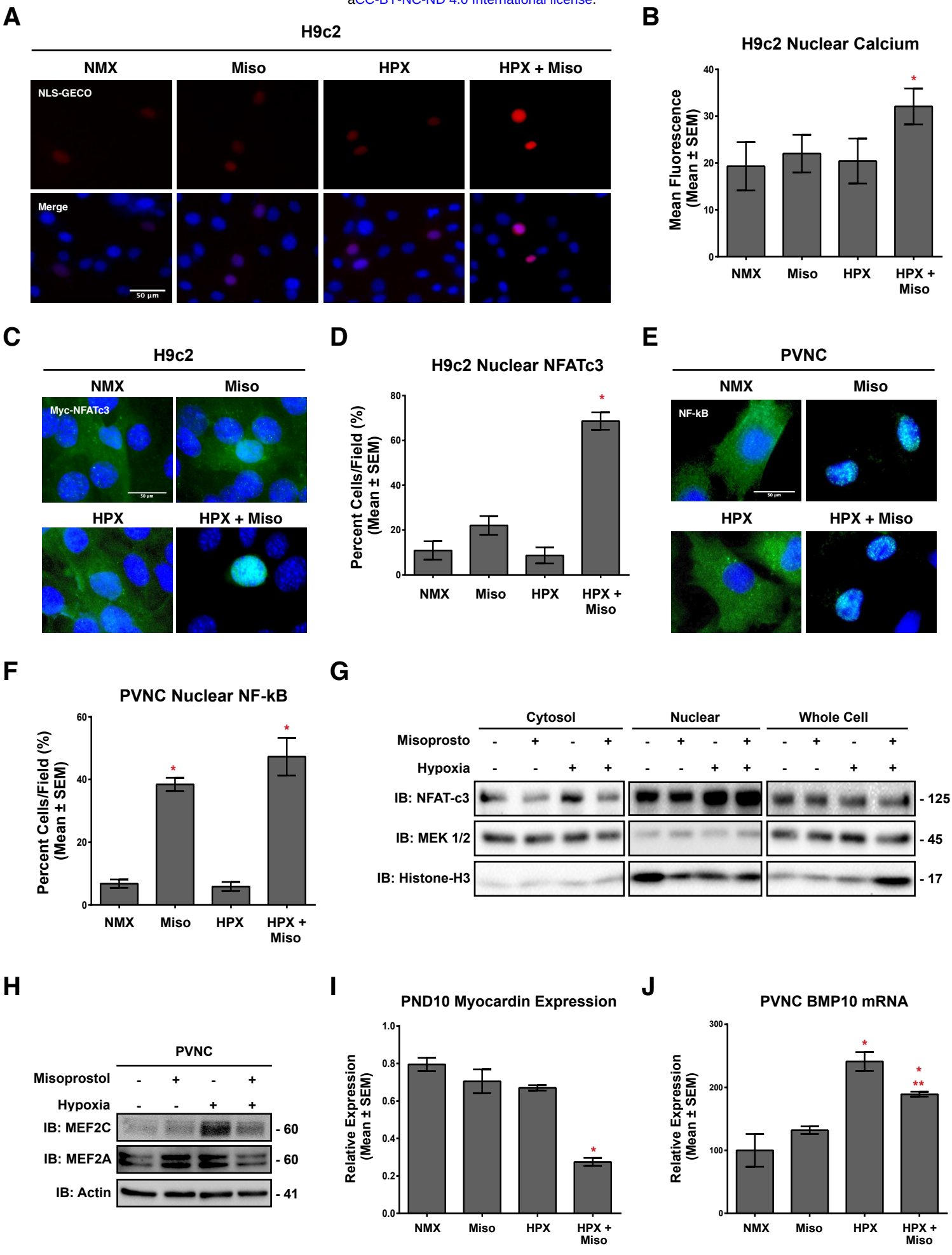

Figure 3

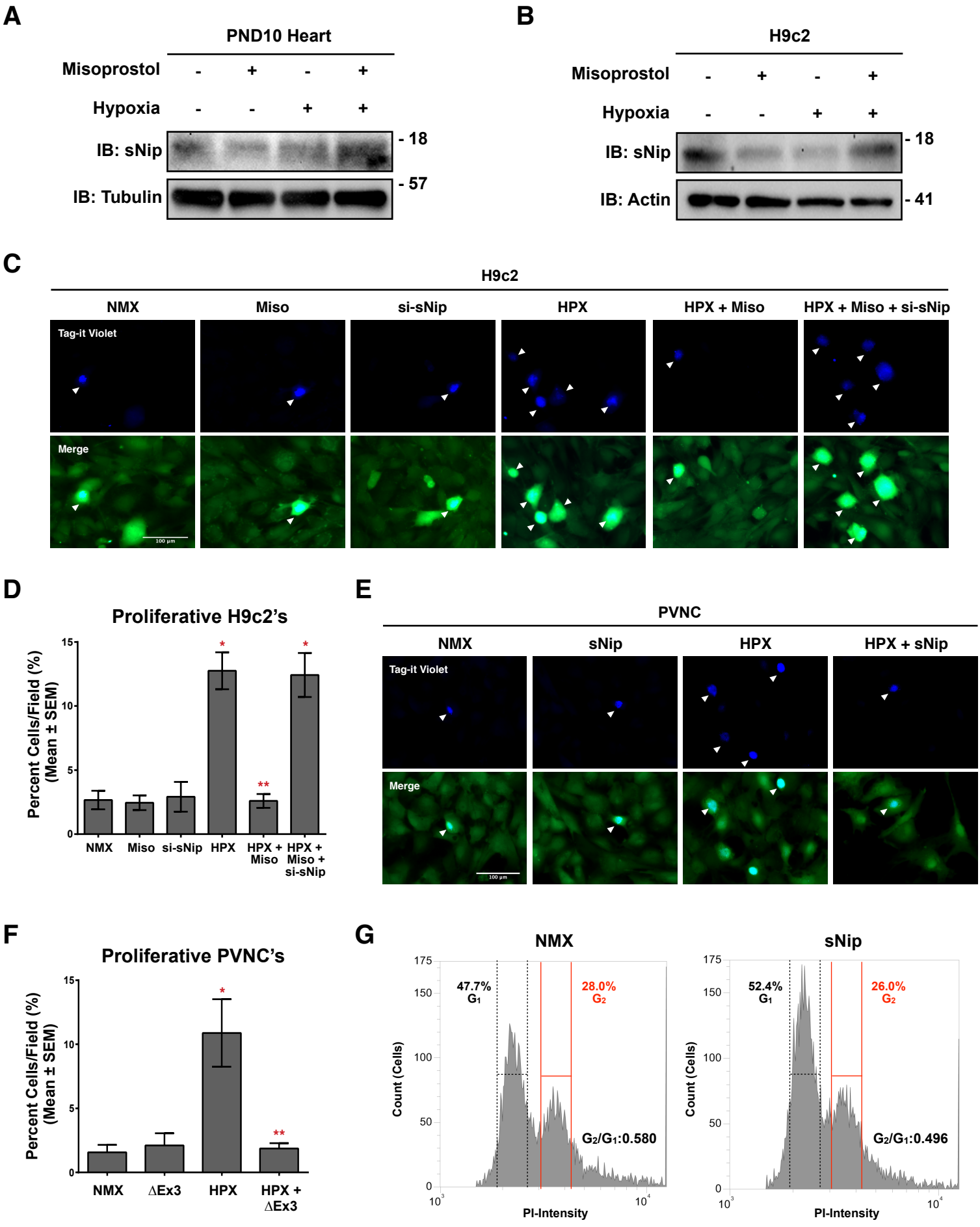

Figure 4